Chemical Engineering Journal 150 (2009) 114–121

Contents lists available at ScienceDirect

Chemical Engineering Journal

journal homepage: www.elsevier.com/locate/cej

# Adsorption of cations on nanofiltration membrane: Separation mechanism, isotherm confirmation and thermodynamic analysis

S.S. Madaeni*, E. Salehi

*Membrane Research Center, Chemical Engineering Department, Razi University, Tagh Bostan, Kermanshah 67149, Iran*

ARTICLE INFO

*Article history:*
Received 24 September 2008
Received in revised form
24 November 2008
Accepted 3 December 2008

*Keywords:*
Membrane
Adsorption
Isotherm
Thermodynamic
Separation mechanism

ABSTRACT

In this research, the adsorption mechanism of the saturated brine cations ($Fe^{2+}$, $Mg^{2+}$ and $Ca^{2+}$) on the negatively charged PVD membrane was investigated. The separation mechanism of the cations was cake deposition on the membrane surface due to adsorption. This was justified on the basis of Hermia blocking laws and surface cake analysis. Three equilibrium adsorption isotherms, Langmuir, Freundlich and Redlich–Peterson were fitted to the quasi-equilibrium adsorption data which were calculated using experimental flux and rejection. The Freundlich and Redlich–Peterson isotherms were found to well represent the measured sorption data on the basis of the acceptable coefficients of determination ($r^2$). An increase in temperature and pressure enhances the adsorption characteristics of the cations. However there are some limitations for pressure increment. For all cations, the significant thermodynamic parameters such as $\Delta G^\circ$, $\Delta H^\circ$ and $\Delta S^\circ$ were calculated, compared and explained on the basis of charge density and hydration radius. The results indicate that the adsorption of cations on the nanofiltration membrane is endothermic and spontaneous due to positive $\Delta H^\circ$ and negative $\Delta G^\circ$. The optimum temperature and pressure for sorption of the cations on PVD membrane were determined as 40 °C and 10 bar, respectively.



## 1. Introduction

The ability of nanofiltration membranes for processing salty solutions is partially based on the presence of chemical functional groups carrying positive or negative charges. This is an interesting technique in many aspects [1,2]. The fouling mechanism of the charged nanofiltration membrane is represented by sieving and electrostatic properties of the membrane [3]. In some cases, the membrane surface charge attracts the solution counter ions and the electrostatic interactions lead to considerable adsorption of particles on the membrane.

The adsorption mechanism and thermodynamic analysis in the field of membrane processes have recently obtained more attention. Mathematical models for adsorption of proteins on affinity membranes were presented using the equilibrium adsorption isotherms [4,5]. These models consider convection, diffusion and adsorption kinetics described by the Langmuir or Freundlich isotherms. The adsorption of papain on the nylon membranes was interpreted with pseudo-second-order kinetic models like Freundlich adsorption isotherm [6]. The adsorption-transport mechanisms of sulfate and chloride anions through PVD membrane were interpreted by the current authors [7] using both Langmuir and Freundlich isotherms. The thermodynamic analysis of adsorption indicates the feasibility and spontaneity of the adsorption process. This has been performed in previous studies [5,6]. A precise identification of the thermodynamic parameters such as $\Delta G^\circ$, $\Delta H^\circ$ and $\Delta S^\circ$ for adsorption leads to optimization of operating conditions such as temperature and pressure for removing the impurities from the solutions. However intensive membrane fouling due to high adsorption potential is a major limitation. Flux may be diminished to a critical value due to high adsorption on the membrane surface.

There is a strong motivation for finding a technique that allows in situ measurement of the adsorption properties of the membranes [8]. For interpretation of the sorption from binary or ternary metal solutions both mono-component and multi-component isotherms were employed. The results show the mono-component models are easy to use and successfully predict metal ions sorption from the multi-metal systems [9,10].

In the current study separation mechanism, isotherms and thermodynamic analysis for adsorption of metal cations on the negatively charged nanofiltration PVD membrane were investigated. Two-parameter equilibrium adsorption isotherms, Langmuir and Freundlich and a three-parameter isotherm, Redlich–Peterson were employed to fit the sorption data at three pressures of 8, 10 and 15 bar and three temperatures of 20, 30 and 40 °C. The effects of temperature and pressure on adsorption mechanism of cations were determined. The thermodynamic parameters of cation adsorption on the membrane were calculated and compared.

* Corresponding author. Tel.: +98 912 2045410; fax: +98 831 4274542.
*E-mail address:* smadaeni@yahoo.com (S.S. Madaeni).

1385-8947/$ – see front matter © 2008 Elsevier B.V. All rights reserved.
doi:10.1016/j.cej.2008.12.005

## 2. An overview of adsorption isotherms

### 2.1. The Langmuir model

The Langmuir adsorption isotherm [11] is the most widely used for adsorption of a pollutant from a liquid solution given the following hypothesis:

- The adsorbed layer is one molecule thick (monolayer adsorption).
- Adsorption occurs at homogeneous sites within the adsorbent.
- Adsorptional energy is constant and does not depend on the degree of occupation of an adsorbent's active centers.
- All sites are identical and energetically equivalent.
- The adsorbent is structurally homogeneous.
- There is no interaction between molecules adsorbed on neighboring sites.

The Langmuir equation is represented as:

$$q = q_s \frac{kc}{1 + kc} \quad (1)$$

where $q$ is equilibrium adsorbed amount per dry adsorbent mass (mg/g), $q_s$ is the final adsorbed amount (mg/g), $c$ is the adsorbate equilibrium concentration in solution (mg/l) and $k$ is a constant reflecting the affinity of the membrane for the metal ions.

### 2.2. The Freundlich model

The empirical Freundlich isotherm [9,12] is used to describe the multilayer adsorption with interaction between molecules, on a heterogeneous sorbent surface. This isotherm can be expressed as:

$$q = kc^m \quad (2)$$

where $q$ is sorption at equilibrium (mg/g), $c$ is the residual ion concentration at equilibrium (mg/l), $k$ is the relative sorption capacity and $m$ is an indicator of sorption intensity or surface heterogeneity. The value of $m$ indicates the degree of non-linearity between solution concentration and adsorbed phase as follows: if $m$ is equal to unity, the adsorption is linear; if the value is below unity, this implies that the adsorption process is chemical and the surface is relatively homogeneous; if the value is above unity, adsorption is a physical process and the sorbent is relatively heterogeneous. In recent case, the sorption favorability and the adsorption site's homogeneity increased, approaching $m$-value to unit.

### 2.3. The Redlich–Peterson model

Redlich–Peterson [12] is a three-parameter empirical equation which may be used to represent adsorption equilibria over a wide concentration range and can be applied either in homogeneous or heterogeneous systems. This isotherm is represented by

$$q = \frac{kc}{1 + bc^m} \quad (3)$$

where $k$ and $b$ are isotherm constants and $m$ is an exponent which indicates the non-linearity of the adsorption systems. Eq. (3) is simplified to the Freundlich isotherm at high adsorbed concentration and to the Langmuir isotherm when $m = 1$.

## 3. Materials and methods

### 3.1. Feed

Saturated brine was used as the feed. This solution was obtained from Cholor-Alkali Unit in Emam Khominei Seaport Petrochemical Plant (Iran). The pH of the solution was in the range of 8.5–9. The concentrations of various solutes available in the solution are presented in Table 1. Physical properties of the ions in the feed are depicted in Table 2 [13,14].

**Table 1**
The concentrations of different solutes in the feed.

| Solute | Concentration |
|---|---|
| NaCl | 290 g/l |
| $SO_4^{2-}$ | 8.0 g/l |
| $Mg^{2+}$ | 9.2 mg/l |
| $Ca^{2+}$ | 8.2 mg/l |
| $Fe^{2+}$ | 0.8 mg/l |

**Table 2**
Physical properties of the ions in the feed [13,14].

| Ion | Ionic radius (nm) | Hydration radius (nm) | Hydration enthalpy (kJ/mol) |
|---|---|---|---|
| $Na^+$ | 0.095 | 0.365 | 418 |
| $Cl^-$ | 0.181 | 0.347 | 338 |
| $SO_4^{2-}$ | 0.23 | 0.38 | 1138 |
| $Mg^{2+}$ | 0.065 | 0.429 | 1923 |
| $Ca^{2+}$ | 0.1 | 0.349 | 1653 |
| $Fe^{2+}$ | 0.055 | 0.435 | 1981 |

### 3.2. Analysis

Concentrations of $Na^+$, $Fe^{2+}$, $Ca^{2+}$ and $Mg^{2+}$ were determined by Atomic Absorption Spectrophotometry (AA-6300 Shimadzu). $SO_4^{2-}$ and $Cl^-$ analysis were performed using Ionic Chromatography (761 Compact IC, Metrohm).

### 3.3. Membrane

PVD (hydranuatics) polymeric membrane was employed for experiments. Characteristics of the membrane are presented in Table 3 [7,14].

### 3.4. Experimental set-up

Fig. 1 depicts the schematic of the experimental set-up. In the experimental trails, the cross-flow batch concentration process method was selected. It means that permeate flow was taken out of the loop and retentate flow was completely returned to the tank. For this purpose a high-pressure pump was employed. On the other hand, pipelines and fittings including the cell, which holds the membrane, must be able to tolerate high pressure. Characteristics of the pump were: $Q_{max}$ = 480 l/h, $P_{max}$ = 80 bar, $T_{max}$ = 50 °C. Excluding some parts of the line that were stainless steel, other parts were high-pressure hoses. The system consisted of a valve to control the applied pressure by the pump and a by-pass valve. These valves were used to control the flow and the pressure. The cell consisted of two cubic parts and was made of a specific alloy. A membrane with the area of 0.0023 $m^2$ was sandwiched between two parts. There were two ducts connected to two hoses. One of these hoses was the feed inlet and the other was retentate out let. The rectangular

**Table 3**
Characteristics of PVD membrane [7,14].

| | |
|---|---|
| Membrane | PVD |
| Skin material | Polyethylene terphetelete |
| Support material | Bis(phenol A polysulfone) |
| Surface characteristic | Smooth |
| Support characteristic | Coarse fiber |
| Membrane structure | Two layer |
| Mass per sheet (g) | 0.76 |
| Thickness (μm) | 150 |

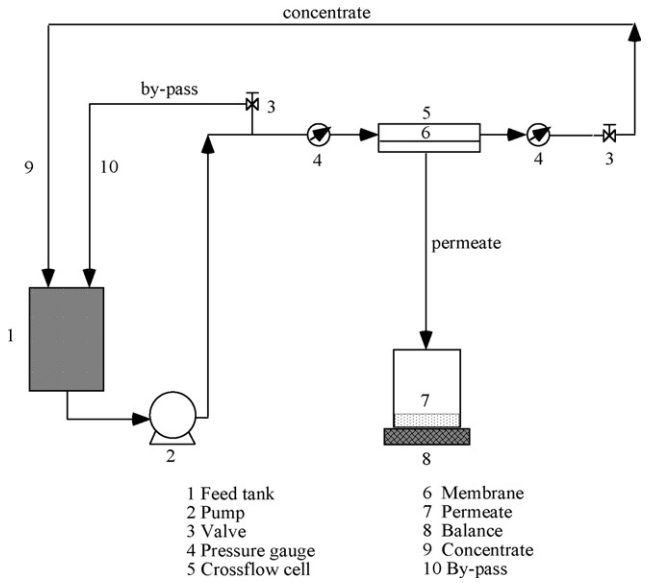


**Fig. 1.** Schematic diagram of the experimental set-up. (1) Feed tank, (2) pump, (3) valve, (4) pressure gauge, (5) cross-flow cell, (6) membrane, (7) permeate, (8) balance, (9) concentrate and (10) by-pass.

membrane was cut exactly to cover the whole area of the pool in one part of the cell. This part had three holes at the bottom to exit the permeate flow out of the cell. The membrane settled on a resistant compact foam layer to protect it against deformation and displacement. Upper part and lower part of the cell were exactly symmetrical and have the same dimensions. After putting the foam into the pool of the lower side, the membrane placed to cover the foam. An o-ring was placed between two parts of the cell.

In the flow line there were two oil pressure gauges (0–60 bar) to show the pressure of concentrated phase before and after the cell. The tank was a plastic vessel with the capacity of 10 l. There was a by-pass before the feed inlet to recycle extra feed to the tank. There were two valves in the by-pass flow and retentate flow to adjust the main flow rate and desired operating pressure.

### 3.5. Filtration procedure

Before starting the experiments, the membrane was soaked in 50% water–ethanol mixture for 10 min. For the first experiments the feed was poured into the tank and filtrate at 40 °C and 8 bar for 210 min. The other measures were performed similarly at different pressures and temperatures. Samples of permeate collected every 30 min to follow variation in permeate flux. Analysis of the permeate samples for each solute was the basis for evaluation of the rejection (*rej*) using:

$$rej\ (\%) = \left(1 - \frac{c_p}{c_0}\right) \times 100 \quad (4)$$

where $c_p$ and $c_0$ represent the solute concentration in permeate and feed, respectively.

## 4. Results and discussion

The cations rejection curves at $T = 40$ °C and three pressures are depicted in Figs. 2–4. The results at $P = 8$ bar and three temperatures are presented in Figs. 5–7. The flux curves at different pressures and temperatures are shown in Figs. 8 and 9. Rejection was increased and flux was decreased during all trials as expected in pressure-driven including nanofiltration process.

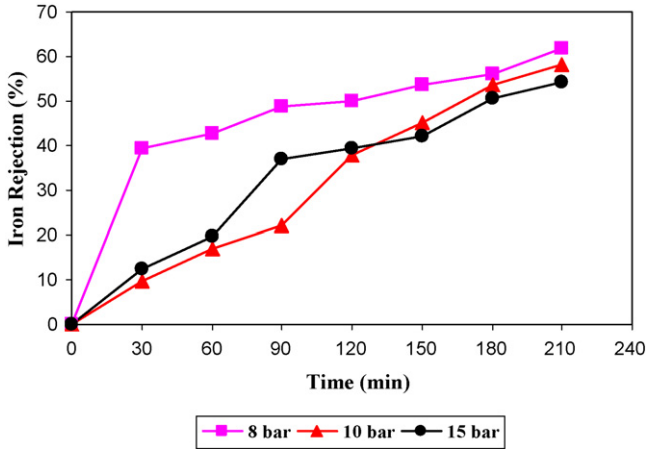


**Fig. 2.** The rejection of the PVD membrane for $Fe^{2+}$-ions at 40 °C and different pressures.

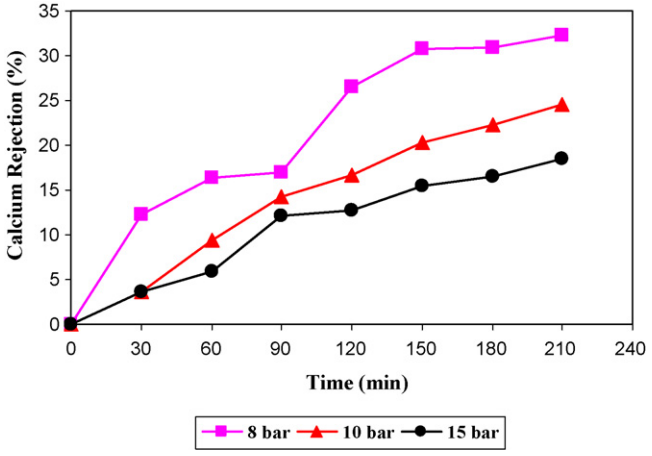


**Fig. 3.** The rejection of the PVD membrane for $Ca^{2+}$-ions at 40 °C and different pressures.

### 4.1. Separation mechanism

The spatial distribution of adsorbed species along the membrane, i.e. membrane surface or internal pores, may be well understood by elucidating the separation mechanisms. Filtration mechanism can be determined using blocking laws [15]. For a mech-

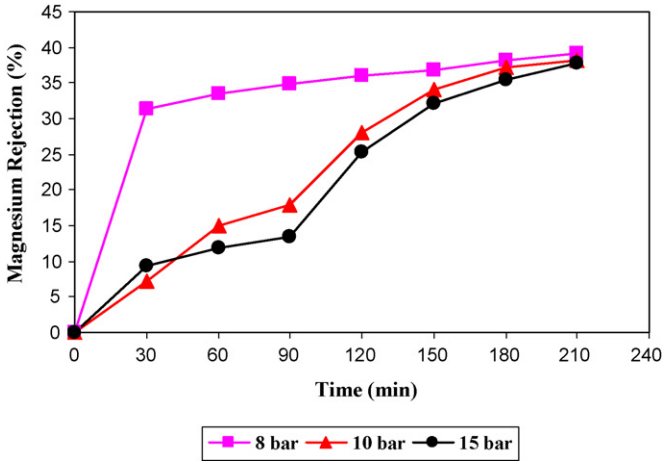


**Fig. 4.** The rejection of the PVD membrane for $Mg^{2+}$-ions at 40 °C and different pressures.

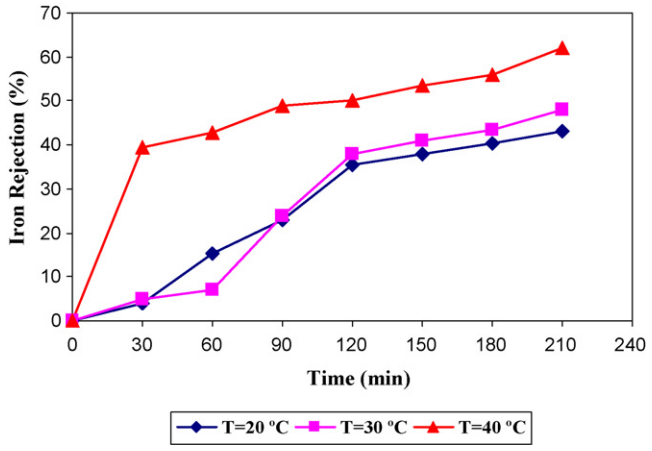


**Fig. 5.** The rejection of the PVD membrane for $Fe^{2+}$-ions at 8 bar and different temperatures.

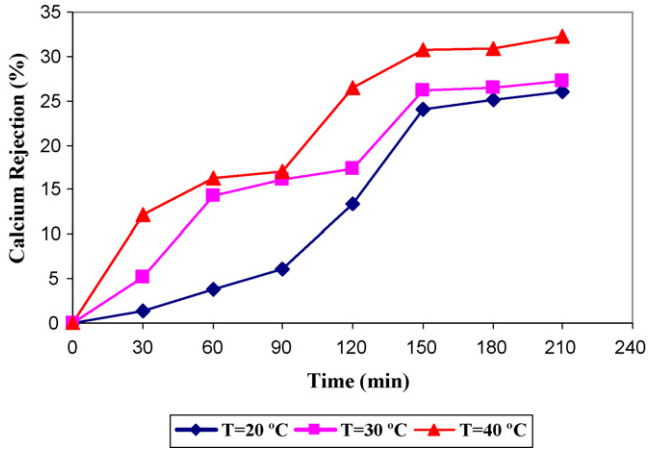


**Fig. 6.** The rejection of the PVD membrane for $Ca^{2+}$-ions at 8 bar and different temperatures.

anism of pore blocking the plot of exp($t$) versus $v$ should be linear. Fore cake (gel) deposition $t/v$ versus $v$ is linear and for internal pore-closure $t/v$ versus $t$ is linear. For filtration of the saturated brine, the plot of exp($t$) versus $v$ is completely non-linear (Fig. 10). The linearity of the plots is the criterion for interpretation of filtration behavior. However this should be coupled with other evidences

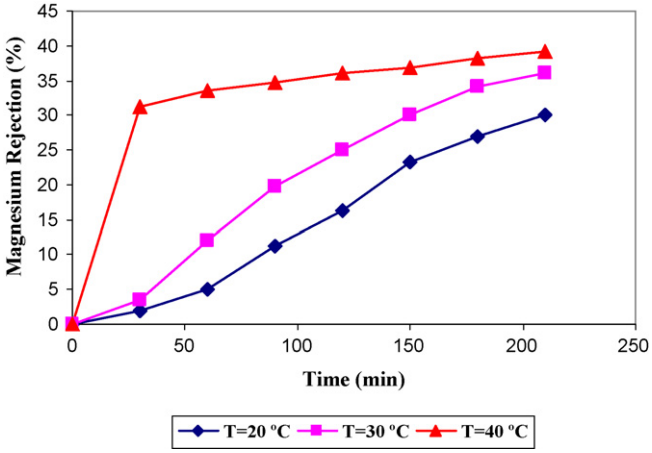


**Fig. 7.** The rejection of the PVD membrane for $Mg^{2+}$-ions at 8 bar and different temperatures.

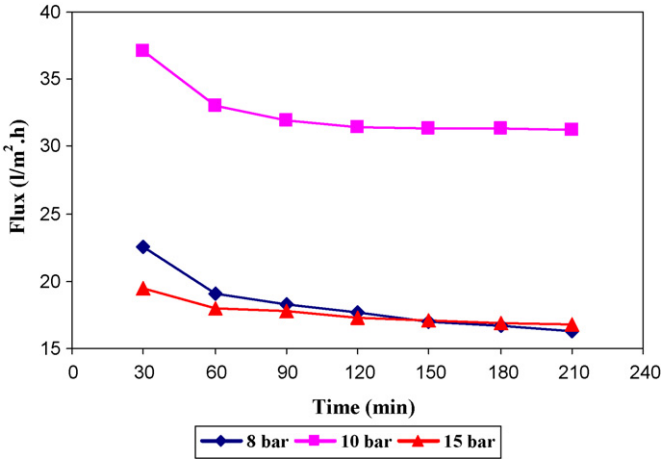


**Fig. 8.** The flux of the PVD membrane at 40 °C and different pressures.

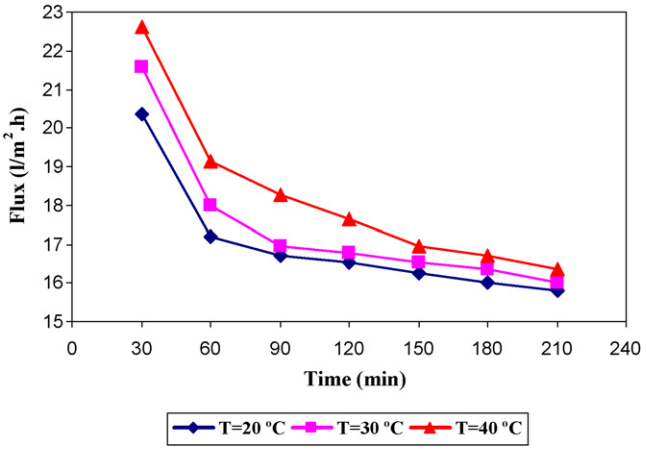


**Fig. 9.** The flux of the PVD membrane at 8 bar and different temperatures.

for elucidation of the mechanism. The plots of $t/v$ versus time and permeate volume are almost linear (Figs. 11 and 12), i.e. cake deposition, internal pore-closure or both may be the dominant filtration mechanism for separation of available ions in the solution using membranes. For further illustration of the filtration mechanism, the analysis of the surface cake or other observations may be employed.

The cations in the solution; $Fe^{2+}$, $Ca^{2+}$ and $Mg^{2+}$, are strongly adsorbed on the negatively charged membrane surface due to the

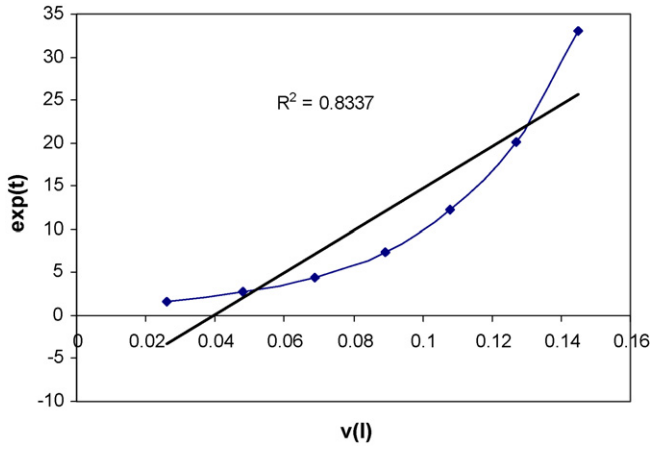


**Fig. 10.** Mechanism determination of saturated brine using PVD membrane (exp($t$) versus $v$).

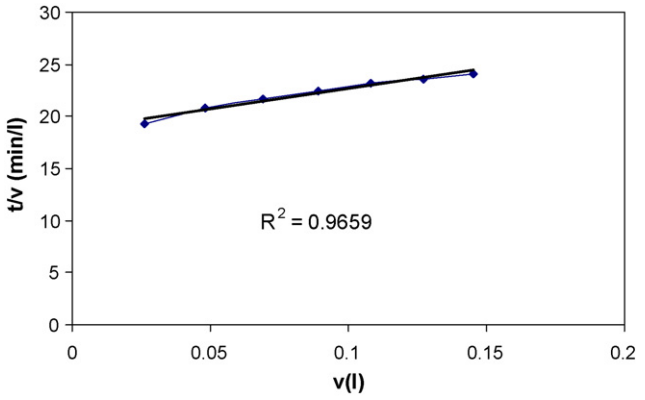


**Fig. 11.** Mechanism determination of saturated brine using PVD membrane ($t/v$ versus $v$).

electrostatic attraction. In another study from the current authors [14], an orange cake formed on the membrane surface was analyzed. Data confirmed the presence of $Fe(OH)_3$ in the deposition. The published reports [14,16] indicate that $Fe^{2+}$-ions compel other cations in the solution to deposit on the membrane surface. This means, the separation mechanism for cations; $Fe^{2+}$, $Ca^{2+}$ and $Mg^{2+}$, is cake deposition on the membrane surface. The superior linearity of $t/v$ versus $v$ plot confirms this conclusion. The negative surface charge of the membrane is covered due to the deposition of the cations. This phenomenon is called "screen phenomenon" [7,16,17]. Therefore, the anions can easily enter into and pass through the membrane without any noticeable electrostatic interactions [7]. Furthermore, low rejection of anions observed during filtration indicates that anions mainly enter into the membrane and cross it to appear in the output permeate. Consequently, the internal pore-closure is the filtration mechanism for separation of anions in the solution. The acceptable linearity of $t/v$ versus $t$ plot as the other proper alternative for filtration mechanism confirms this conclusion. Table 1 clearly shows that NaCl has the most concentration (about 97%) among the available ions in the solution. Accordingly the passage of $Na^+$ ions through the membrane is a requisite for passing $Cl^-$-ions due to the electron neutrality of permeate. A summary of the above discussion is presented in Table 4.

### 4.2. Isotherms confirmation

Available cations in the solution encountering the membrane are assumed to be in quasi-equilibrium with the cations in the adsorbed phase. The latter is formed on the membrane during the

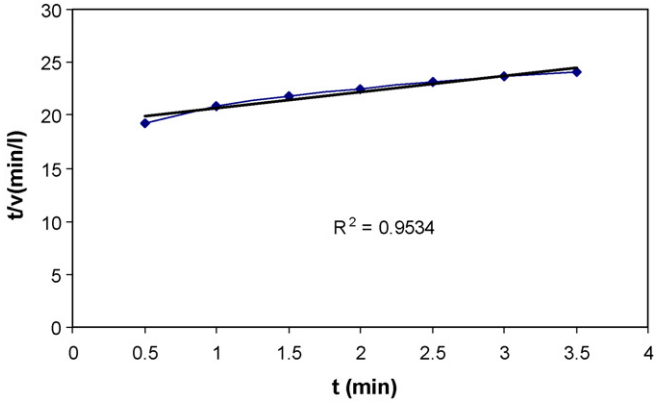


**Fig. 12.** Mechanism determination of saturated brine using PVD membrane ($t/v$ versus $t$).

**Table 4**
Filtration mechanism of the ions in the system.

| Ion | Separation mechanism |
|---|---|
| $Mg^{2+}$, $Fe^{2+}$, $Ca^{2+}$ | Surface cake formation (due to adsorption) |
| $Cl^-$ | Internal pore-closure |
| $Na^+$ | Internal pore-closure (due to electron neutrality) |
| $SO_4^{2-}$ | Internal pore-closure |

filtration process. In fact, a very long term is required to establish a real thermodynamic equilibrium in the system. The adsorption on the membrane surface was realized as the dominant mechanism for separation of cations from the solution. Therefore, we tested and adjusted the equilibrium parameters for three isotherms; Langmuir, Freundlich and Redlich–Peterson, using the experimental rejection and flux data. Every 30 min a portion of the process time ($\Delta t$) was assumed to be an "adsorption stage". The amount of ions adsorbed in one adsorption stage was defined as $n_{si}$ (mg):

$$n_{si} = rej_i c_0 F_i A \Delta t \quad (i = 1, 2, 3, \ldots) \tag{5}$$

Here $i$ is the stage counter, $A$ is the membrane area in contact with the flow stream ($m^2$), $F_i$ is the permeate flux ($l/(m^2\,h)$), $c_0$ is the initial cation concentration in the solution (mg/l or ppm) and $rej_i$ is average cation rejection at any adsorption stage. The amount of each cation adsorbed from the beginning to the $i$th stage of the filtration process was defined as $n_i$ (mg):

$$n_i = n_{i-1} + n_{si} \quad (n_0 = 0,\ \ i = 1, 2, 3, \ldots) \tag{6}$$

The equilibrium adsorbed cation per unit mass of the membrane ($M_m$) was indicated as $Q_e$ (mg/g):

$$Q_e = \frac{n_i}{M_m} \tag{7}$$

The approximate cation's concentration which is in equilibrium with the adsorbed phase was defined as $C_e$ (ppm):

$$C_e = c_0 - c_{pi} \tag{8}$$

where $c_{pi}$ is the permeate concentration in the $i$th stage of the process.

The isotherms fitting results for $Fe^{2+}$-ion at three pressures are depicted in Figs. 13–15. For other cations ($Ca^{2+}$ and $Mg^{2+}$) the fitting data are not shown.

The results for all pressures indicate that both two-parameter Freundlich isotherm and three-parameter Redlich–Peterson

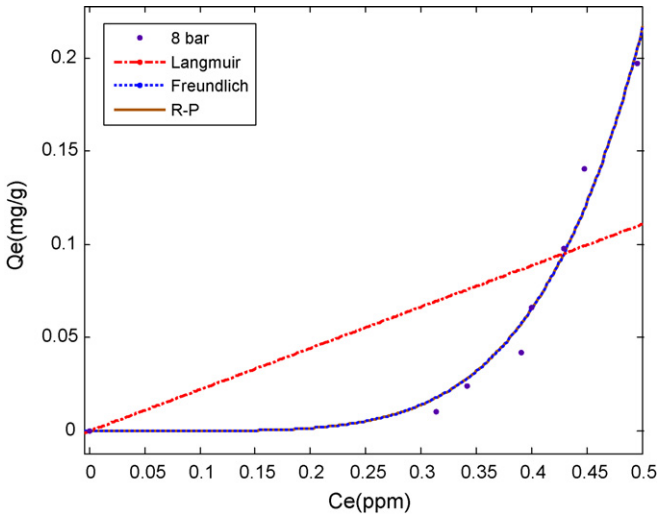


**Fig. 13.** Isotherms for the sorption of $Fe^{2+}$-ions using PVD membrane at pressure 8 bar and 40 °C.

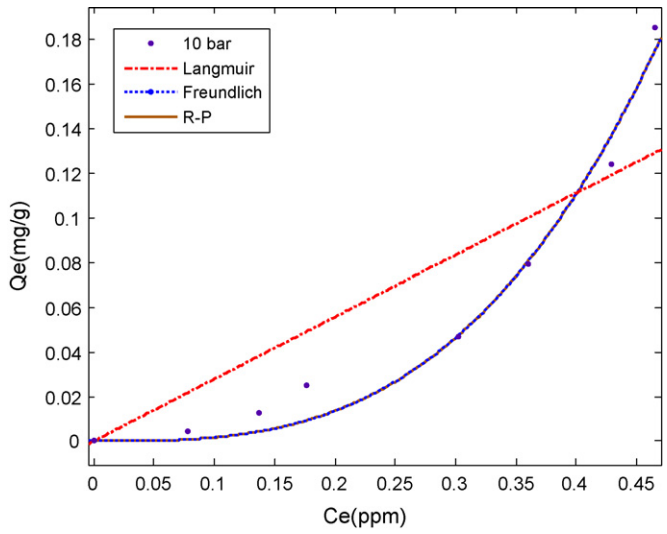


**Fig. 14.** Isotherms for the sorption of $Fe^{2+}$-ions using PVD membrane at pressure 10 bar and 40 °C.

isotherm with acceptable coefficients of determination ($r^2$) are able to properly interpret the adsorption mechanism of the cations. However in some cases the fitting accuracy of the Freundlich isotherm is slightly improved. Frequently R–P isotherm partially overlaps the Freunlich isotherm. The Langmuir isotherm is not fitted into the equilibrium data. Based on the isotherm fitting results, it seems that multilayer adsorption of cations on PVD membrane and the interaction between adsorbed cations should be considered for process elucidation. The *m*-value of the Freundlich isotherm is above unity. This means the sorption of cations may be a physical process and the membrane adsorption sites are relatively heterogeneous in nature. The equilibrium parameters of Freundlich isotherm for adsorption of cations onto the PVD membrane at 40 °C and three operating pressures are presented in Table 5.

### 4.3. Effect of pressure

The exponent "*m*" in the Freundlich isotherm represents the heterogeneity in the adsorption process. This parameter shows the

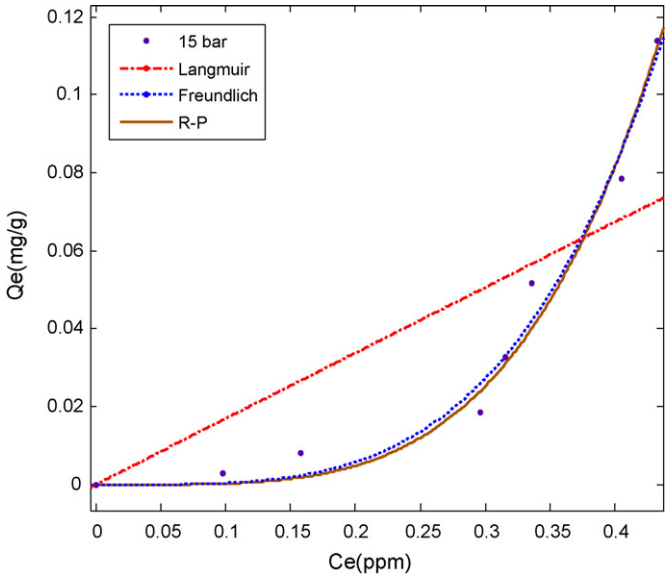


**Fig. 15.** Isotherms for the sorption of $Fe^{2+}$-ions using PVD membrane at pressure 15 bar and 40 °C.

**Table 5**
Freundlich isotherm's equilibrium parameters at different pressures and 40 °C.

| Cation | $Fe^{2+}$ | $Ca^{2+}$ | $Mg^{2+}$ |
|---|---|---|---|
| 8 bar | $k = 8.661$<br>$m = 5.335$ | $k = 3.36 \times 10^{-6}$<br>$m = 10.1$ | $k = 0.00236$<br>$m = 5.82$ |
| 10 bar | $k = 1.778$<br>$m = 3.031$ | $k = 0.0348$<br>$m = 4.661$ | $k = 0.0667$<br>$m = 3.602$ |
| 15 bar | $k = 1.776$<br>$m = 3.025$ | $k = 0.0062$<br>$m = 3.861$ | $k = 0.0641$<br>$m = 3.015$ |

differences in energy distribution of active adsorption sites which leads to heterogeneous distribution of adsorbed species on the surface. Larger "*m*" indicates higher difference in energy and capability of active sites for adsorption. This means greater heterogeneity.

The factor (*m*) is decreased with pressure increment (from 8 to 15 bar) in cross-flow filtration of saturated brine using PVD nanofilter at 40 °C (Fig. 16) leading to a decline in heterogeneity and an improvement in homogeneous nature of adsorption of cations on the membrane surface. However for establishment of a general pattern indicating the effect of pressure on adsorption heterogeneity extensive experimental data are required. However the observed trend, i.e. decreasing the heterogeneity factor by increasing the pressure from 8 to 15 bar may be justified due to enhancement in the turbulence shear stresses on the adsorbing ions and active adsorption sites on the membrane surface. Moreover the lateral interaction between adsorbing cations may be weakened leading to higher attraction of species toward the active sites of the membrane surface. Accordingly greater homogeneous sorption may be occurred at higher pressures.

The accommodation accuracy of the Freundlich isotherm ($r^2$) is increased by pressure up to 10 bar and is decreased afterward using three operating pressure as depicted in Fig. 17. The highest fitting of Freundlich adsorption isotherm at 10 bar means that 'adsorption' may be the most dominant mechanism using membrane compared to the other possible separation mechanisms including screening, sieving, drag forces (or inertia) and electrostatic exclusion. The shear stress on the cations may be improved with increasing pressure from 8 to 10 bar. The excess pressure at 10 bar forces the cations to proceed closer to the membrane and presumably adsorb on the surface by adsorptional electrostatic potential field. By further pressure increment (from 10 to 15 bar), the shear stress is probably enhanced with an unfavorable effect on adsorption. The adsorbed cations may easily detach from the membrane surface.

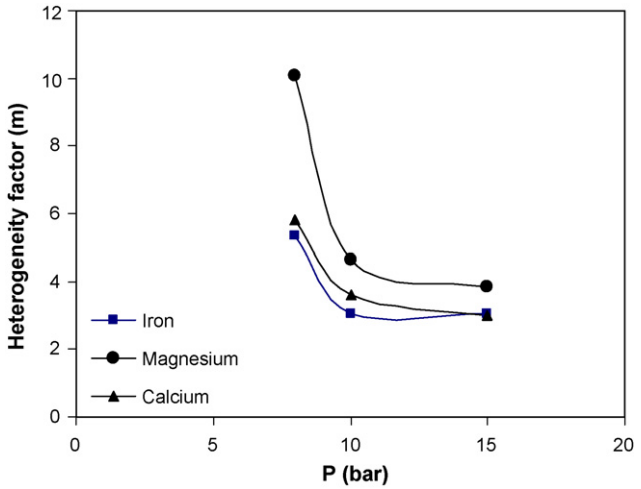


**Fig. 16.** The heterogeneity factor or *m*-value of the Freundlich isotherm versus pressure for the cations.

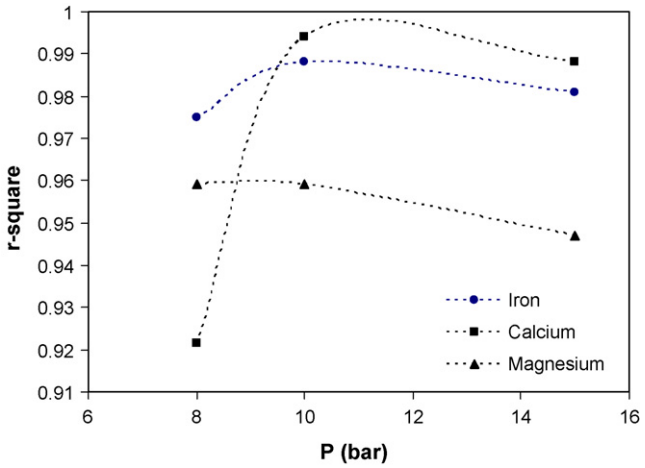


**Fig. 17.** The variations of the coefficient of determination ($r^2$) of the Freundlich isotherm versus pressure for the cations.

Moreover the exposure time of the cations on the membrane which is required to reach to the equilibrium is decreased. However some of the cations may be separated from the solution by the membrane surface due to the appeared shear stress or drag forces at 15 bar.

In qualitative view, the shapes of the isotherms are more like to linear or favorable [12] type at pressure 10 bar which shows further adsorbed amount versus the same ionic concentration at this pressure. Consequently, an intermediate or average value (10 bar) was selected as the optimum operating pressure for adsorption of cations on the PVD nanofiltration membrane.

### 4.4. Thermodynamic analysis

The Gibbs free energy change ($\Delta G^\circ$), indicates the degree of the spontaneity of the adsorption process. For significant adsorption, the free energy changes of adsorption must be negative. The Gibbs free energy change of adsorption is defined as:

$$\Delta G^\circ = -RT \ln K \quad (9)$$

where $R$ is universal gas constant (8.314 J/(mol K)) and $T$ is the absolute temperature. $K$ is the thermodynamic equilibrium constant, which may be obtained from the intercept of $\ln(Q_e/C_e)$ versus $Q_e$ plot [18]. The constant $K$ for adsorption of $Fe^{2+}$-ions onto the PVD membrane is determined by plotting $\ln(Q_e/C_e)$ versus $Q_e$ and extrapolating to zero $Q_e$ at three operating temperatures. The results for $Fe^{2+}$-ion are depicted in Fig. 18 (not shown for the other cations).

The most important thermodynamic parameters, i.e. $\Delta H^\circ$, $\Delta S^\circ$ and $\Delta G^\circ$ are connected by

$$\Delta G^\circ = \Delta H^\circ - T\Delta S^\circ \quad (10)$$

$\Delta H^\circ$ and $\Delta S^\circ$ of adsorption can be determined from the slope and the intercept of the linear plot of $\ln K$ versus $1/T$, respectively. The plot of $\ln K$ versus $1/T$ for $Fe^{2+}$-ions is shown in Fig. 19 (not shown for the other cations). Table 6 presents the thermodynamic parameters of the cations. The positive value of $\Delta H^\circ$ for each cation, suggests the endothermal nature of adsorption. $\Delta G^\circ$ values were negative

**Table 6**
Comparison of thermodynamic parameters for the sorption of metal cations by PVD membrane.

| Cation | $\Delta H^\circ$ (kJ/mol) | $\Delta G^\circ$ (kJ/mol) | $\Delta S^\circ$ (kJ/(mol K)) |
|---|---|---|---|
| $Fe^{2+}$ | 2.3 | −3.0667 | 0.018 |
| $Ca^{2+}$ | 1.172 | −3.1213 | 0.0144 |
| $Mg^{2+}$ | 1.711 | −3.1488 | 0.0163 |

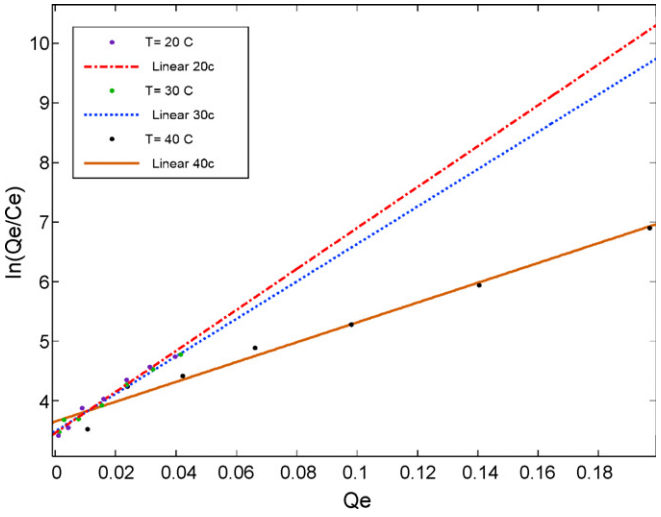


**Fig. 18.** Plots of $\ln(Q_e/C_e)$ versus $Q_e$ for the adsorption of $Fe^{2+}$-ions on the PVD membrane at different temperatures.

indicating the adsorption process led to a decrease in Gibbs free energy. Negative $\Delta G^\circ$ values indicate the feasibility and spontaneity of the adsorption of the cations. The positive values of $\Delta S^\circ$ reflect increasing randomness at solid/liquid interface during the sorption of the cations on the membrane [19].

Comparing the enthalpy and the entropy of adsorption of the cations indicating the following sequence:

$$Fe^{2+} > Mg^{2+} > Ca^{2+}$$

This observation may be justified due to the cation's charge density and hydration intensity. All the cations have similar charges but their ionic radiuses are dissimilar. The charge density of each cation is defined as the charge to size ratio and indicates its hydration tendency. Therefore, the cation's hydration tendency and the released energy of hydration (Table 2) can be compared as follows:

$$Fe^{2+} > Mg^{2+} > Ca^{2+}$$

Along increasing the cations hydration tendency, the cation's effective charge has been screened with more attached water molecules. This results in a decrease in the capability of the membrane electrostatic field to adsorb the cation. In other words adsorption of $Fe^{2+}$ with the highest hydration tendency which screens the effective

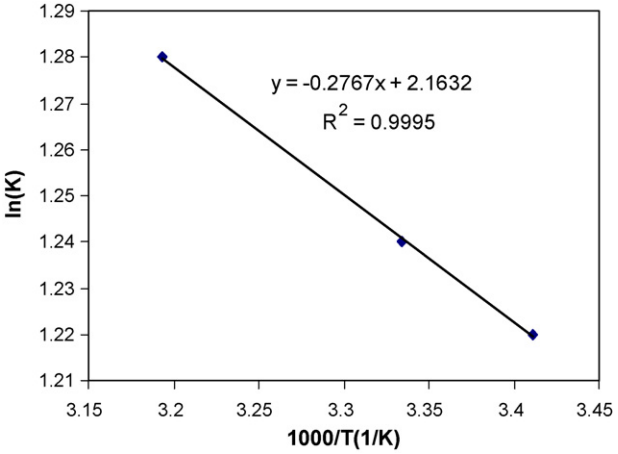


**Fig. 19.** The plot of $\ln K$ versus $1/T$ for adsorption thermodynamic study of $Fe^{2+}$-ions on the PVD membrane.

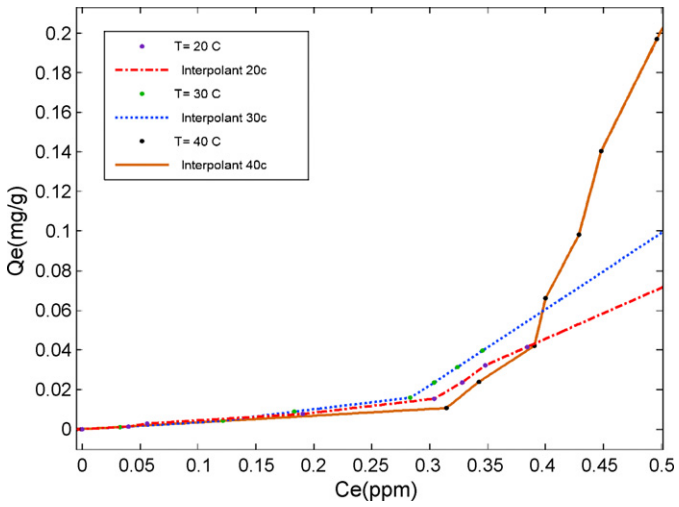


**Fig. 20.** Plots of the adsorption equilibria of the $Fe^{2+}$-ions on the PVD membrane at $P = 8$ bar and different temperatures.

charge; requires the most energy for adsorption, i.e. this cation has maximum adsorption enthalpy.

The hydrated cations carry water molecules toward the membrane surface. These molecules disturb and disarray the adsorbed layer on the membrane surface, i.e. increasing the entropy. In summary, the adsorption entropy is increased by cations with higher charge density and hydration tendency.

### 4.5. The effect of temperature

The cation sorption on the membrane is endothermal in nature ($\Delta H^\circ > 0$). In other words temperature is a favorable parameter, i.e. the final adsorbed amount of each cation is increased with temperature. The effect of temperature on equilibrium adsorption of $Fe^{2+}$ on the PVD membrane is depicted in Fig. 20 using three operating temperatures for calculation of the equilibrium adsorption data. For other cations the same trend was obtained (results are not shown). However the cation's mobility may also be enhanced by increasing the temperature. Disturbing the adsorbed layer due to further ionic movement, results in a decline in the cations sorption at the early stages in the filtration process. A superior cation sorption in this study was obtained at 40 °C among three tested operating temperatures.

## 5. Conclusion

The adsorption of the saturated brine cations ($Fe^{2+}$, $Mg^{2+}$ and $Ca^{2+}$) onto the nanofiltration PVD membrane was investigated. Filtration mechanism was cake deposition due to cation sorption on the membrane. Three isotherms; Langmuir, Freundlich and Redlich–Peterson were fitted to the equilibrium sorption data. The empirical Freundlich and Redlich–Peterson isotherms were the isotherms of choice on the basis of the highest $r$-squares.

The results indicate that an increment in temperature and pressure improves the sorption of the cations. However at pressures higher than 10 bar the isotherm's fitting accuracy is diminished. The positive values of $\Delta H^\circ$ and the negative values of $\Delta G^\circ$ represent the endothermal nature and the spontaneity of cations adsorption. The thermodynamic parameters of the adsorbed cations may be compared on the basis of ionic charge density and hydration intensity.

## References

[1] A.C. Oumar, D. Trebouet, P. Jaouen, Nanofiltration of sea water: fractionation of mono and multi-valent cations, Desalination 140 (2001) 67–77.
[2] B. Vander Breuggen, A. Koninck, C. Vandecasteele, Separation of mono-valent and divalent ions from aqueous solution by electrodialysis and nanofiltration, Journal of Water Resources 38 (2004) 1347–1353.
[3] J.F. Lapointe, Y. Pouliot, C. Bouchard, Fouling of a nanofiltration membrane by a $\beta$-lactoglobulin tryptic hydrolystate: impact on the membrane sieving and electrostatic properties, Journal of Membrane Science 235 (2005) 89–102.
[4] C. Francesca, C.S. Giulio, Adsorption of pure recombinant MBP-fusion proteins on amylose affinity membranes, Journal of Membrane Science 273 (2006) 2–11.
[5] B. Cristiana, S. Dimartino, C.S. Giulio, Modeling and simulation of affinity membrane adsorption, Journal of Chromatography A 1162 (2007) 24–33.
[6] H.L. Nie, T.X. Chen, L.M. Zhu, Adsorption of papain on dye affinity membranes: isotherm, kinetic, and thermodynamic analysis, Separation & Purification Technology 57 (2007) 121–125.
[7] S.S. Madaeni, E. Salehi, Adsorption-transport modeling for transmission of anions through PVD membrane in presence of screen phenomenon, Applied Surface Science 255 (2009) 3523–3529.
[8] T.E. Clark, H.W. Deckman, R.R. Chance, In situ determination of the adsorption characteristics of a zeolite membrane, Journal of Membrane Science 230 (2003) 91–98.
[9] D. Kumar, A. Singh, J.P. Gaur, Mono-component versus binary isotherm models for Cu(II) and Pb(II) sorption from binary metal solution by green alga pithophora oedogonia, Bioresource Technology 99 (2008) 8280–8287.
[10] A.J. Prosser, E.I. Franses, Adsorption and surface tension of ionic surfactants at the air–water interface: review and evaluation of equilibrium models, Colloids and Surfaces A 178 (2001) 1–40.
[11] D.M. Ruthven, Principles of Adsorption and Adsorption Processes, fifth edition, John Wiley & Sons, 1984.
[12] F. Gimbert, N. Morin-Crini, F. Renault, Adsorption isotherm models for dye removal by cationized starch-based material in a single component system: error analysis, Journal of Hazardous Materials 157 (2008) 34–46.
[13] L. Firdaous, F. Quemeneur, J.P. Schlumpf, J.P. Maleriat, Modification of the ionic composition of salt solutions by electrodialysis, Desalination 167 (2004) 397–402.
[14] S.S. Madaeni, V. Kazemi, Treatment of saturated brine in chlor-alkali process using membranes, Separation & Purification Technology 61 (2007) 72–78.
[15] J. Hermia, Constant pressure blocking filtrations laws—application to power-law non-Newtonian fluids, Transactions of the Institute of Chemical Engineers 60 (1982) 183–187.
[16] N.B. Frares, S. Taha, G. Dorange, Influence of the operating conditions on the elimination of zinc ions by nanofiltration, Desalination 185 (2005) 245–253.
[17] M. Soltanieh, M. Mousavi, Application of charged membranes in water softening: modeling and experiments in the presence of polyelectrolytes, Journal of Membrane Science 154 (1999) 53–64.
[18] J. Wu, H.Q. Yu, Biosorption of 2,4-dichlorophenol from aqueous solution by phanerochaete chrysosporium biomass: isotherm, kinetics and thermodynamics, Journal of Hazardous Materials 137 (2006) 498–508.
[19] R.R. Navarro, K. Sumi, N. Fujii, M. Matsumura, Mercury removal from waste water using porous cellulose carrier modified with polyethyleneimine, Journal of Water Research 30 (1996) 2488–2494.